

RED SEA OUTFLOW DURING THE LAST GLACIAL MAXIMUM

E.J. Rohling* and W.J. Zachariasse†

*Department of Oceanography, University of Southampton, Southampton SO17 1BJ, U.K.

†Department of Geology, Institute for Paleoenvironment and Paleoclimate Utrecht (IPPU), Institute of Earth Sciences, Utrecht University, P.O. Box 80.021, 3508 TA Utrecht, The Netherlands

The Red Sea is connected to the Gulf of Aden, and hence to the Arabian Sea, via the Strait of Bab-el-Mandab, which is only about 20 km wide and 300 m deep. The shallowest part of the passage, however, lies about 140 km further basin-inward, near greater Hanish Island. That passage is only 137 m deep, while the channel deeper than 120 m is only 11 km wide. Foraminiferal and isotopic studies suggest that the inflow-outflow salinity contrast at Bab-el-Mandab was about 10 ‰ during the Last Glacial Maximum (LGM), compared with 3.1 ‰ at present. Calculation of maximal outflow during the LGM suggests that it was about 14% of the present-day value, while the density of this outflow was around 1035 kg m⁻³, compared to the modern value of about 1029 kg m⁻³. Therefore, it seems very likely that this outflow played no role of importance in the intermediate water ventilation of the Arabian Sea during the LGM. The Persian Gulf influence on this ventilation may be excluded as well, since the very shallow Persian Gulf was completely above sea level during the LGM. It is anticipated that, among other influences, LGM curtailment of these sources for intermediate depth ventilation should be reflected in the intensity and extent of the Oxygen Minimum Zone (OMZ) in the Arabian Sea. Other sources may have become important, such as northward penetration of Antarctic Intermediate Water. The Institute for Paleoenvironment and Paleoclimate Utrecht has recently participated in the 1992 Netherlands Indian Ocean Expedition, with the intention to determine Late Quaternary variations in the intensity and extent of the Arabian Sea OMZ in transects of cores recovered across its lower depth limit.

INTRODUCTION

In the Red Sea (Fig. 1), strong excess of evaporation over freshwater input results in a net water deficit of about 2 m year⁻¹, and a mainly salinity-related increase in density

within the Red Sea (Siedler, 1969; Morcos, 1970; Grasshoff, 1975). This drives a distinct anti-estuarine circulation in the Red Sea with inflow of surface water from the adjacent Gulf of Aden, and subsurface return flow of dense water into that basin. In summer, this pattern is complicated by wind-

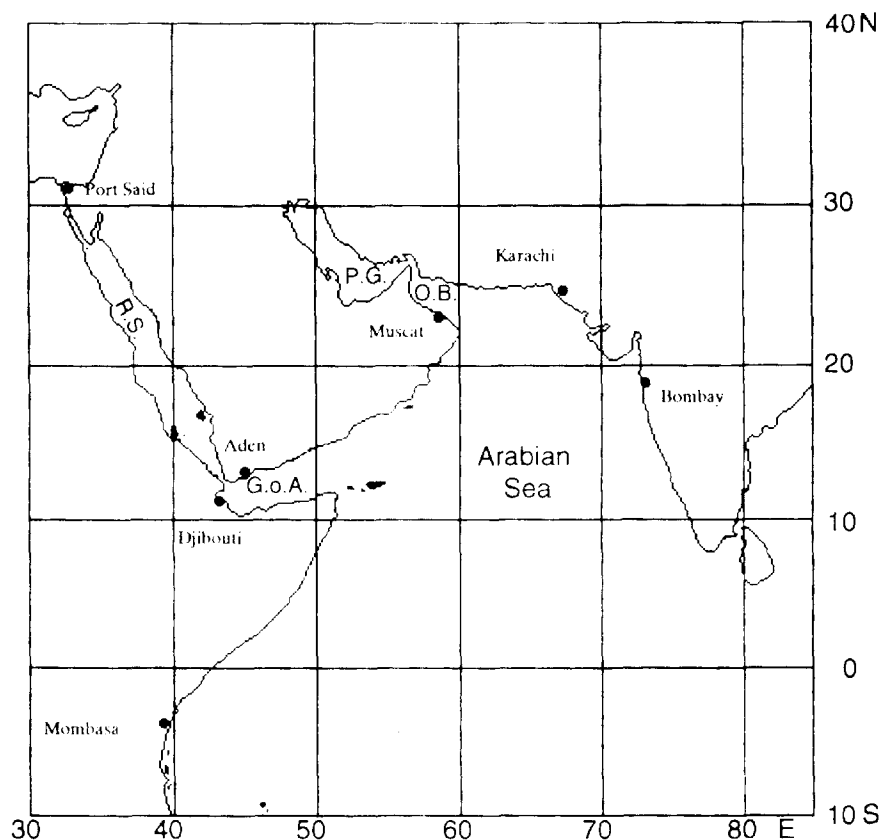


FIG. 1. Map of the area discussed in this paper. R.S. is the Red Sea, G.o.A. the Gulf of Aden, P.G. the Persian Gulf, and O.B. the Oman Basin.

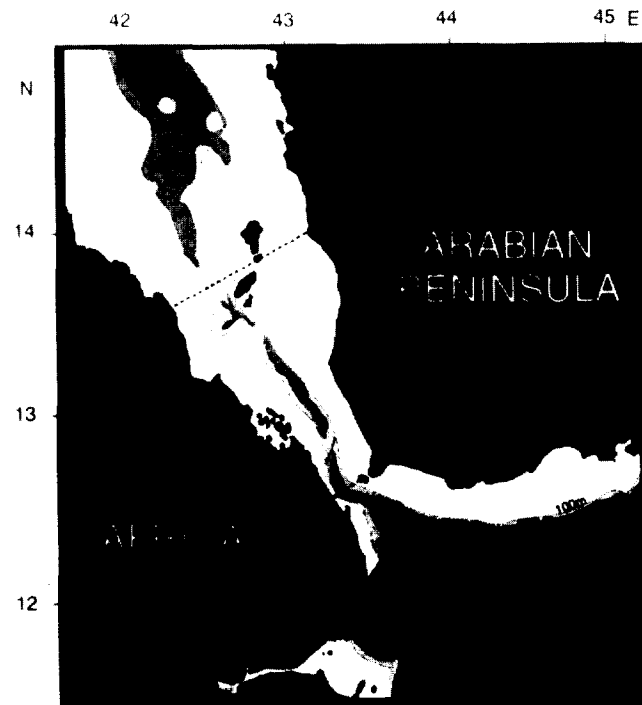


FIG. 2. Map of the passage between Red Sea and Gulf of Aden. N. refers to the narrowest passage near Perim Island, and S to the shallowest passage near Hanish Island (after Werner and Lange, 1975). Depth contours in metres.

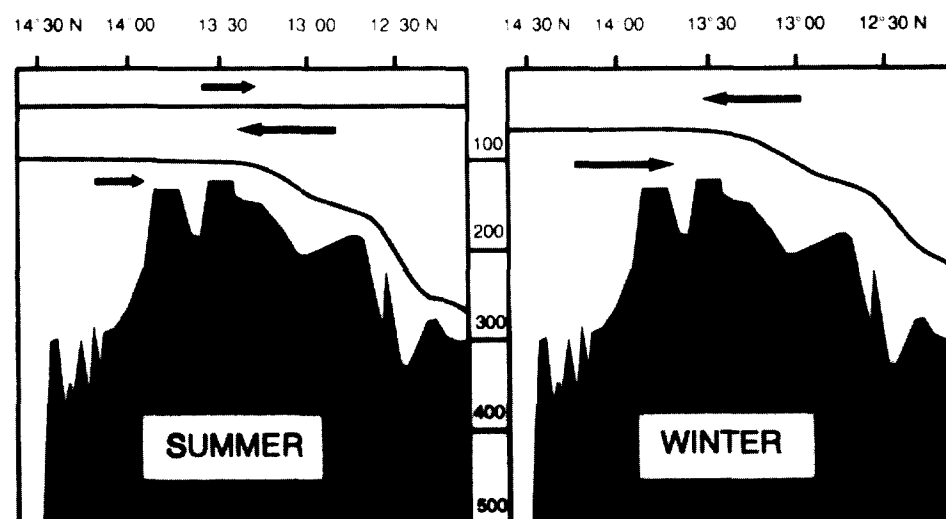


FIG. 3. Schematic along-strait profiles, showing the modern summer and winter circulation patterns through the Strait of Bab-el-Mandab (after Thompson, 1939; Patzert, 1974a, b; Maillard and Soliman, 1986; Souvermezoglou *et al.*, 1989). Depth scale in metres.

induced reversal of the flow through the strait at the very surface (< 40 m), while inflow at intermediate levels and outflow at depth continue (Figs 2, 3) (Thompson, 1939; Patzert, 1974a, b; Maillard and Soliman, 1986; Souvermezoglou *et al.*, 1989).

The above-described exchange is most evident in the Strait of Bab-el-Mandab, the connection between the Red Sea and the Gulf of Aden (Figs 2, 3 after Rohling, 1994). The narrowest passage is located near Perim Island, where the main channel is only about 20 km wide, and about 300 m deep. Some 140 km basin-inwards, just east of Hanish Island, the passage is shallowest but much wider. There it has a maximum depth of 137 m (Werner and Lange, 1975), and a width of about 105 km. It is emphasized that this

passage is deeper than 120 m only over a width of about 11 km. During the Last Glacial Maximum (LGM), assuming 120 m sea-level lowering (Fairbanks, 1989), therefore, the passage would have been only 11 km wide and about 17 m deep.

The present-day Red Sea surface area is about 4.4×10^{11} m². With a net water deficit of about 2 m year⁻¹, therefore, the volume of present-day excess evaporation (X^p) is about 8.8×10^{11} m³ year⁻¹ (p indicates present-day value) (Siedler, 1969). According to conservation of mass and salt arguments, the volume of subsurface outflow of Red Sea water (V_{rs}) is calculated as $V_{rs} = (S_{ga} X)/S$, where S_{ga} is the salinity of surface inflow from the Gulf of Aden, and S the outflow–inflow salinity contrast. With $S_{ga}^p = 36.6$, and $S^p =$

3.1, V_{rs}^p is about $104 \times 10^{11} \text{ m}^3 \text{ year}^{-1}$, or 0.33 Sv (Siedler, 1969).

The dense outflow from the Red Sea consists of water with remarkably low oxygen concentrations (Neumann and McGill, 1962). Although this water was in relatively recent contact with the atmosphere, which would have enabled saturation with oxygen, its high temperature and salinity prevented oxygen concentrations from reaching high values like those found in intermediate or deep waters formed in cold regions. Furthermore, Neumann and McGill (1962) demonstrated a strong intermediate depth oxygen minimum layer in the Red Sea that intensifies from north to south, suggesting rapid oxygen consumption especially in the southern part of the basin. Most of the dense Red Sea outflow originates from this oxygen-depleted layer, and reaches the Gulf of Aden with oxygen concentrations mostly below 1.50 ml l^{-1} (Grasshoff, 1975). The waters below the surface mixed layer in the Gulf of Aden that mix with the Red Sea outflow contain even lower oxygen concentrations of 0.75 ml l^{-1} or less (Grasshoff, 1975).

The influence of dense subsurface outflow from the Red Sea can be traced throughout the Arabian Sea between about 300 and 900 m (Morcos, 1970; Wyrki, 1973; Tchernia, 1980). Shapiro and Meschanov (1991) show that the waters originating from the Red Sea spread predominantly towards the south and east when leaving the Gulf of Aden. A northward branch is also present, but it is much less pronounced. Red Sea water may be recognized as far south as $20\text{--}25^\circ\text{S}$ in the Mozambique Channel, where it reaches depths around 1100 m (Wyrki, 1971; Gründlingh, 1985).

Another source of intermediate water in the Arabian Sea is the dense outflow from the Persian Gulf (mean depth about

25 m; Tchernia, 1980). The Persian Gulf (Fig. 1) contributes to the intermediate water ventilation of the Arabian Sea at relatively shallow levels (150–300 m), especially in the northernmost part of the Arabian Sea (Morcos, 1970; Wyrki, 1973; Tchernia, 1980; Shapiro and Meschanov, 1991). The volume of outflow from the Persian Gulf is about half of that from the Red Sea (Tchernia, 1980). Morcos (1970) summarized the conclusions of a substantial number of early studies on the spread of Red Sea and Persian Gulf water in the Arabian Sea. He emphasized that it is more appropriate to talk of water from Red Sea + Gulf of Aden, and from Persian Gulf + Gulf of Oman, when discussing the origin of intermediate water masses in the NW Indian Ocean, since intensive mixing with surrounding waters occurs immediately after the subsurface flows leave the Red Sea and Persian Gulf. This mixing dilutes the original properties of the outflow, while the original volume is augmented manifold by entrainment of surrounding waters.

Figures 4, 5 and 6 illustrate the vertical structure of the Arabian Sea observed in two CTD casts from R.V. Tyro during the Netherlands Indian Ocean Program (NIOP) of 1992, directly off the Gulf of Aden and in the Gulf of Oman, respectively. Distinct plumes of high salinity Red Sea + Gulf of Aden water ($S = 35.6$ to 35.8 , $T = 12$ to 14°C), were found between about 300 and 750 m depth (Fig. 5; Van der Weijden *et al.*, 1992). In the Oman Basin (northernmost part of the Arabian Sea), a much shallower plume was found between 200 and 300 m, consisting of Persian Gulf + Gulf of Oman water ($S = 36.2$, $T = 17^\circ\text{C}$; Fig. 6; Van der Linden *et al.*, 1992).

During the Last Glacial Maximum (LGM), when sea level stood about 120 m below its modern position (Fairbanks,

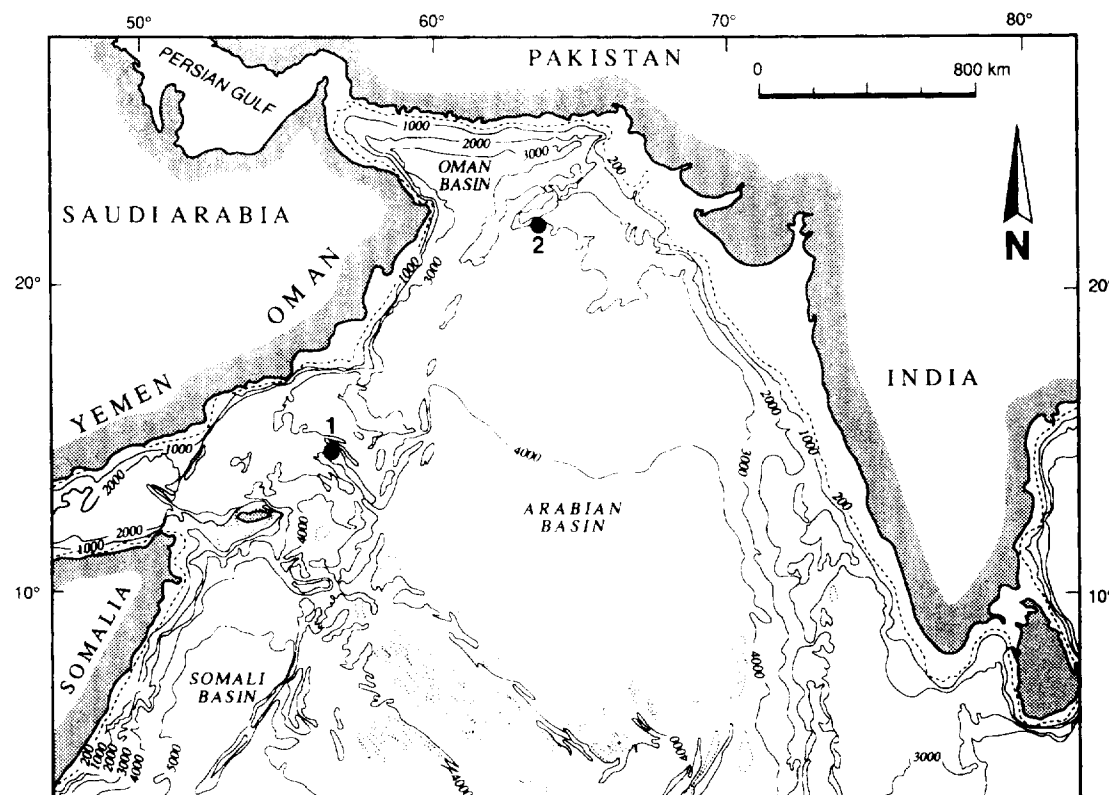


FIG. 4. Locations of the CTD casts from R.V. Tyro during the NIOP'92 expedition portrayed in Figs 5 and 6. Number 1 refers to station 498, number 2 to station 458.

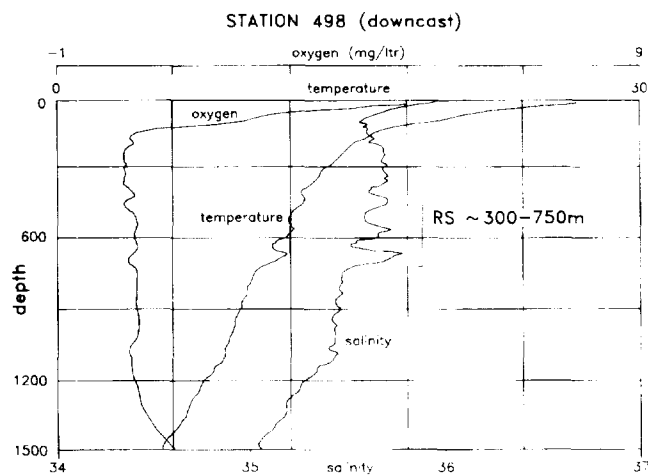


FIG. 5. Plot of temperature, salinity, and oxygen concentration against depth in CTD station 498 off the Gulf of Aden (after Van der Weijden *et al.*, 1992).

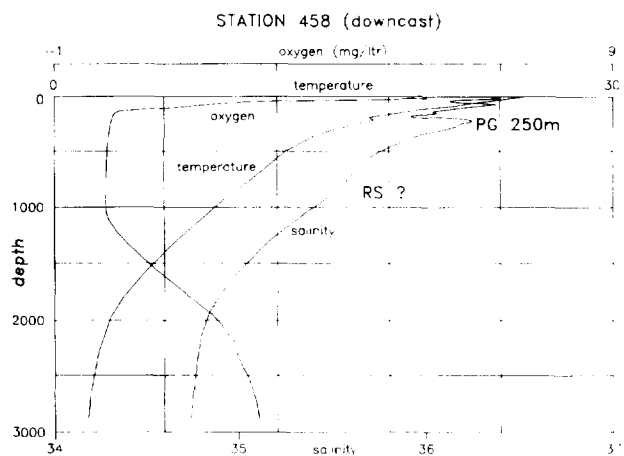


FIG. 6. Plot of temperature, salinity and oxygen concentration against depth in CTD station 458, Oman Basin (after Van der Linden *et al.*, 1992).

1989), the Persian Gulf was completely emerged. Therefore, it may be excluded as a source-area for ventilation of the Arabian Sea intermediate water during full glacial times, and probably remained unimportant until sea level had risen to about -25 m (around 9000 BP; Fairbanks, 1989).

The amount of Red Sea outflow during the LGM may be assessed by calculating the maximal outflow over the shallowest passage between Red Sea and Gulf of Aden by assuming that the Froude number for outflow achieved a critical value of 1 at the sill (this paper; after Rohling, 1994). Another constraint that can be made concerns the Red Sea surface area during the LGM, since the elimination of large shelf areas by a 120 m lowering of sea level would have reduced that surface area by about 50% (Locke, 1986). Values for inflow salinity and outflow salinity determined from fossil evidence then complete the set of estimates necessary to speculate on the influence of Red Sea outflow on ventilation of the Arabian Sea at intermediate depth during the LGM. This is the scope of the present paper, which provides background to the participation of IPPU in the Netherlands Indian Ocean Program of 1992.

GLACIAL CONDITIONS

During the LGM, the summer SW monsoon was substantially weakened, and the winter NE monsoon intensified (Duplessy, 1982; Van Campo *et al.*, 1982; Fontugne and Duplessy, 1986). In combination with the drastic sill depth reduction by 120 m glacial sea level lowering (Fairbanks, 1989), weakening of the summer monsoon would have resulted in far less pronounced seasonal reversal of surface flow in the Strait of Bab-el-Mandab. Therefore, the glacial exchange between the Red Sea and Gulf of Aden may safely be considered as two-layered.

As mentioned before, the Strait of Bab-el-Mandab is narrowest on the outward (Gulf of Aden) side, and shallowest on the inward (Red Sea) side. Considering the influence of strait geometry on exchange transport, the Bab-el-Mandab configuration allows for a simple model focusing entirely on the shallowest passage, since the narrowest width of a passage will only influence the exchange if it occurs between the sill and the reservoir containing the denser fluid (Farmer and Armi, 1986).

During the LGM, 120 m of sea-level lowering (Fairbanks, 1989) would have left a passage across the Hanish Sill only 17 m deep, and about 11 km wide. Calculation of maximal outflow may then be performed by assuming that the Froude number for outflow achieved a critical value of one at the sill (Farmer and Armi, 1986; Bryden and Kinder, 1991), giving, $U_{rs}^2 = 0.375 g'H$ where U_{rs} is the outflow velocity; $g' = g\Delta\rho/\rho_{rs}$; g is gravitational acceleration; $\Delta\rho$ is the outflow-inflow density contrast; ρ_{rs} is the density of subsurface Red Sea outflow; H is sill depth. Since $g' \approx 7.4 \times 10^{-3} \Delta s$, this idealization gives maximum estimate $U_{rs}^{LGM} = 0.22 \text{ m} \sqrt{\Delta s^{LGM} \Delta}$, so that $V_{rs}^{LGM} = 15428 \sqrt{\Delta s^{LGM}} \text{ m}^3 \text{ s}^{-1} (\approx 4.9 \times 10^{11} \sqrt{\Delta s^{LGM}} \text{ m}^3 \text{ yr}^{-1})$.

ΔS^{LGM} may be estimated from the fossil record. During the LGM, planktonic foraminifera hardly survived in the Red sea, resulting in the presence of the so-called a-planktonic zone in Red Sea cores, which is characterized by low abundances or sometimes even absence of planktonic foraminifera (e.g. Locke, 1986). In this interval, only two species have been found, albeit in (very) low abundances, namely the warm euryhaline mixed layer dweller *Globigerinoides ruber*, and the cosmopolitan species *Globigerinita glutinata* (Berggren and Boersma, 1969; Ivanova, 1985; Locke, 1986; Locke and Thunell, 1988). According to their salinity tolerances, the absence of *Globigerinoides sacculifer* and *Globigerinella siphonifera* (upper limit about $S = 47$; Hemleben *et al.*, 1989) and the persistence of *Globigerinoides ruber* (upper limit about $S = 49$; Hemleben *et al.*, 1989) in the glacial Red Sea suggest that $S_{rs}^{LGM} \approx 48$, or $\Delta S^{LGM} \approx 10$. A similar estimate of ΔS^{LGM} has been obtained by comparing changes in the $\delta^{18}\text{O}$ records from the Red Sea and Gulf of Aden (Thunell *et al.*, 1988). In the northernmost parts of the Red Sea, salinities may have risen to exceed 50 ppt (Reiss *et al.*, 1980; Winter, 1983; Almogi-Labin *et al.*, 1986), which may have happened in the central Red Sea as well (Almogi-Labin *et al.*, 1991). The inferred high glacial salinity is supported by the presence of chemical precipitates and benthic foraminiferal species indicative of

hypersaline conditions, in the LGM interval of Red Sea cores (Ku *et al.*, 1969; Milliman *et al.*, 1969; Halicz and Reiss, 1981; Winter *et al.*, 1983; Locke, 1986; Almogi-Labin *et al.*, 1986; Locke and Thunell, 1988).

Using $\Delta S^{lgm} \approx 10$, $S_{ga}^{lgm} \approx 37.6$, and $V_{rs}^{lgm} \approx 4.9 \times 10^{11} \sqrt{\Delta S^{lgm}} \text{ m}^3 \text{ year}^{-1}$, $X = (V_{rs} \Delta S) / S_{ga}$ gives $X^{lgm} \approx 4.1 \times 10^{11} \text{ m}^3 \text{ year}^{-1}$. This is about half of the present value of excess evaporation. The total surface area of the Red Sea at glacial times, however, was also reduced to about half of its present value, so that the above calculation suggests that the net water deficit during the LGM was roughly equal to the present (about 2 m year^{-1}).

DISCUSSION AND CONCLUDING REMARKS

Today, there are no major rivers draining into the Red Sea, and there is less than 100 mm year^{-1} of precipitation (Pedgley, 1974; Grasshoff, 1975). Hence, the total freshwater input compensates for no more than 5% of the water evaporated each year, so that it may be considered negligible. It is not surprising that the glacial water deficit was so similar to that of today because, the freshwater input being so small, X is essentially the rate of evaporation. If the net water deficit during the LGM was quite similar to the modern deficit, then sea-surface temperature, which predominantly determines the rate of evaporation, should also have been quite similar to the present. This is endorsed by previous studies suggesting that glacial temperatures in the NW Indian Ocean were about 2°C lower than today (CLIMAP, 1976, 1981; Prell *et al.*, 1980).

With the salinity of Red Sea outflow during the LGM near 48‰, the density of this outflow would have ranged between the incredibly high values of about 1036 and 1035 kg m^{-3} (for temperatures between 15 and 20°C), compared to 1029.5 and 1028.5 kg m^{-3} at present. The volume of outflow would, according to the above calculation, have been as small as 14% of the present. These numbers suggest that glacial Red Sea outflow was of no likely importance to the ventilation of intermediate waters of the Arabian Sea. Rather, its high density should have caused the Red Sea outflow to settle deep in the basin. Furthermore, the small volume of outflow probably makes its influence in the open Arabian Sea virtually undetectable by means of fossil evidence. Obviously, further study is needed to check on this speculation, and especially cores from isolated depressions in the deep Gulf of Aden may show the influence of high salinity/density Red Sea outflow water during the LGM. With respect to the open Arabian Sea, Zahn and Pedersen (1991) noted the absence of a typical Red Sea signature at intermediate depths during the LGM, endorsing the results of the calculations made in this paper.

With respect to the intermediate depth ventilation of the Arabian Sea during the LGM, we conclude that both the Red Sea and Persian Gulf sources were shut down. This would have eliminated not only the salinity maxima between 200 and 900 m that characterize the Arabian Sea at present, but also the input of oxygen (little as it may be) at intermediate depth from these source areas. As a result, the severe Arabian Sea Oxygen Minimum Zone (OMZ) which is presently

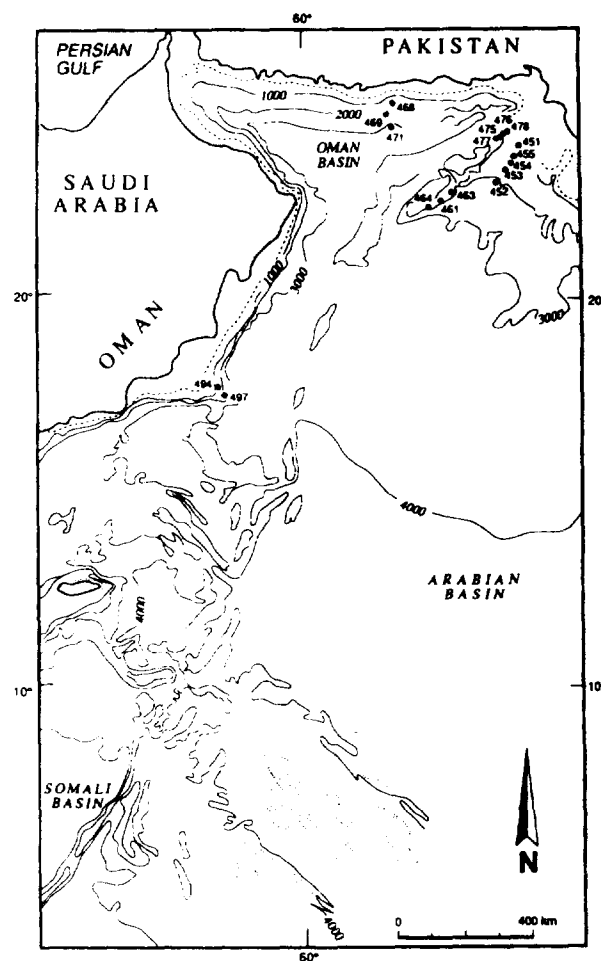


FIG. 7. Location-map of selected box-cores recovered with R.V. Tyro during the NIOP'92 expedition.

found between about 150 and 1200 m (Figs 5 and 6), may have been intensified during the LGM by reduction of lateral oxygen advection. In that case, vertical expansion of the OMZ may be expected. On the contrary, however, reduced upwelling in the Arabian Sea during the LGM (a.o. Anderson and Prell, 1991; Niitsuma *et al.*, 1991; Shimmiel and Mowbray, 1991) would have reduced mid-depth oxygen consumption, so that the extent of the OMZ may have been equal to the present, or even somewhat decreased. Even more complicating, the intermediate depths of the glacial NW Indian Ocean may have been filled with waters from a presently unimportant source, perhaps by northward penetration of the cold, low-saline, oxygen-rich (3.0 ml l^{-1} at 10°S ; Tchernia, 1980) Antarctic Intermediate Water (AAIW). Zahn and Pedersen (1991) stated that their glacial $\delta^{18}\text{O}$ and $\delta^{13}\text{C}$ data from the Oman margin may be suggestive of such a northward penetration of AAIW, which today is retained south of a hydrological front at 10°S . In that case, the intensity and extent of the glacial OMZ may have been severely reduced. To discriminate between these alternatives (or some other), new research is required, since as yet very little is known about variations in the intermediate depths of the Arabian Sea.

During the NIOP'92 expedition, seventeen boxcores were selected from those recovered across the base of the OMZ in the northeastern Arabian Sea (Fig. 7). Changes in modern

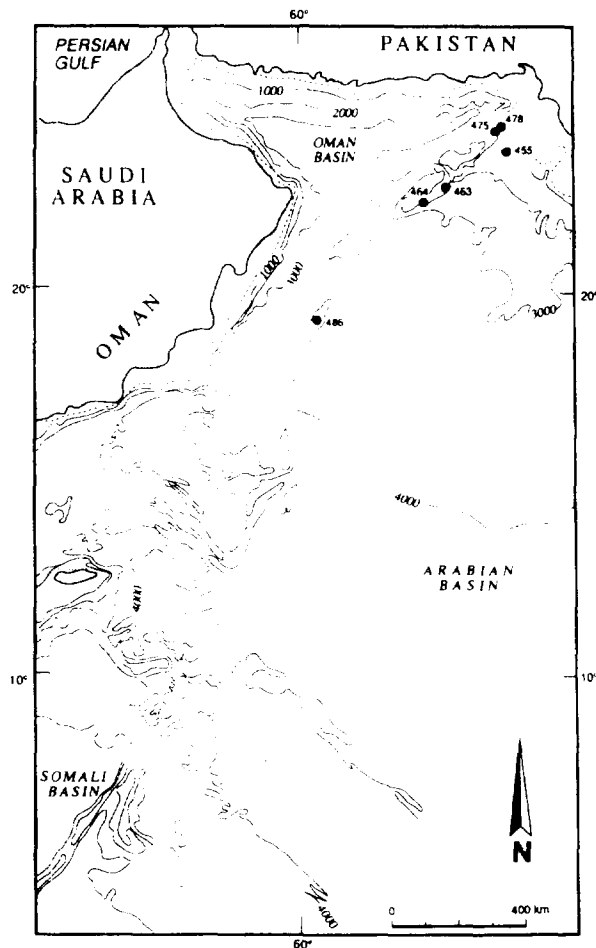


FIG. 8. Location-map of selected piston cores recovered with R.V. Tyro during the NIOP'92 expedition.

benthic foraminiferal faunas associated with this level will be used in piston core studies to portray possible vertical changes in the lower depth limit of the OMZ during the last two glacial cycles (for locations of the selected piston cores, see Fig. 8). The results will be placed in a more general paleoceanographic framework using stable isotopes, planktonic foraminifera, dinoflagellates, and geochemical tracers, while sedimentological studies concentrate on the influence of Indus river discharge.

ACKNOWLEDGEMENTS

Thanks are due to H. Bryden, W.W. Hay and R.C. Thunell for discussions, assistance and valuable suggestions, and to W.J.M. Van der Linden and C.H. Van der Weijden, the chief scientists of Legs 2 and 3 of the NIOP'92 expedition, respectively. This study is part of project VvA of the Netherlands Organisation for Scientific Research (NWO), and provides a written account of a presentation to the IUGS-UNESCO CLIP-Project meeting in Holetown, Barbados in November 1993.

REFERENCES

- Almogi-Labin, A., Luz, B. and Duplessy, J.C. (1986). Quaternary paleoceanography, pteropod preservation and stable-isotope record of the Red Sea. *Palaeogeography, Palaeoclimatology, Palaeoecology*, **57**, 195–211.
- Almogi-Labin, A., Hemleben, C., Meischner, D. and Erlenkeuser, H. (1991). Paleoenvironmental events during the last 13,000 years in the central Red Sea as recorded by pteropoda. *Paleoceanography*, **6**, 83–98.
- Anderson, D.M. and Prell, W.L. (1991). Coastal upwelling gradient during the Late Pleistocene. *Proc. O.D.P., Scientific Results*, **117**, 265–281.
- Berggren, W.A. and Boersma, A. (1969). Late Pleistocene and Holocene planktonic foraminifera from the Red Sea. In: Degens, E.T. and Ross, D.A. (eds). *Hot Brines and Recent Heavy Metal Deposits in the Red Sea*. pp. 282–298. Springer, Berlin.
- Bryden, H.L. and Kinder, T.H. (1991). Steady two-layer exchange through the Strait of Gibraltar. *Deep-Sea Research*, **38**, 445–463.
- CLIMAP Project Members (1976). The surface of the ice-age Earth. *Science*, **191**, 1131–1137.
- CLIMAP Project Members (1981). Seasonal reconstruction of the earth's surface at the last glacial maximum. *Geological Society of America M-C36*.
- Duplessy, J.C. (1982). Glacial to interglacial contrasts in the northern Indian Ocean. *Nature*, **295**, 494–498.
- Fairbanks, R.C. (1989). A 17,000 year glacio-eustatic sea level record: influence of glacial melting rates on the Younger Dryas event and deep-ocean circulation. *Nature*, **342**, 637–642.
- Farmer, D.M. and Armi, L. (1986). Maximal two-layer exchange over a sill and through the combination of a sill and contraction with barotropic flow. *Journal of Fluid Mechanics*, **164**, 53–76.
- Fontugne, M.R. and Duplessy, J.C. (1986). Variations of the monsoon regime during the Upper Quaternary: evidence from carbon isotopic record of organic matter in north Indian ocean sediment cores. *Palaeogeography, Palaeoclimatology, Palaeoecology*, **56**, 69–88.
- Grasshoff, K. (1975). The hydrochemistry of landlocked basins and fjords. In: Riley, J.P. and Skirrow, G. (eds), *Chemical Oceanography*, Vol. 2, pp. 455–597. Academic Press, London.
- Gründlingh, M.L. (1985). Occurrence of Red Sea water in the southwestern Indian Ocean. *J. Physical Oceanography*, **15**, 207–212.
- Halicz, E. and Reiss, Z. (1981). Paleocological relations of foraminifera in a desert-enclosed sea — The Gulf of Aqaba. *Marine Ecology*, **2**, 15–34.
- Hemleben, Ch., Spindler, M. and Anderson, O.R. (1989). *Modern Planktonic Foraminifera*. Springer, New York, 363 pp.
- Ivanova, E.V. (1985). Late Quaternary biostratigraphy and paleotemperatures of the Red Sea and Gulf of Aden based on planktonic foraminifera and pteropods. *Marine Micropaleontology*, **9**, 335–364.
- Ku, T.L., Thurber, D.L. and Mathieu, G.G. (1969). Radiocarbon chronology of Red Sea sediments. In: Degens, E.T. and Ross, D.A. (eds), pp. 348–359. *Hot Brines and Recent Heavy Metal Deposits in the Red Sea*, Springer, Berlin.
- Locke, S.M. (1986). The paleoceanographic record of the last glacial/interglacial cycle in the Red Sea and Gulf of Aden, Thesis, Univ. South Carolina, Columbia, S.C., 97 pp.
- Locke, S.M. and Thunell, R.C. (1988). Paleoceanographic record of the last glacial/interglacial cycle in the Red Sea and Gulf of Aden. *Palaeogeography, Palaeoclimatology, Palaeoecology*, **64**, 163–187.
- Maillard, C. and Soliman, G. (1986). Hydrography of the Red Sea and exchanges with the Indian Ocean in summer. *Oceanologica Acta*, **9**, 249–269.
- Milliman, J.D., Ross, D.A. and Ku, T.L. (1969). Precipitation and lithification of deep-sea carbonates in the Red Sea. *J. Sedimentary Petrology*, **39**, 724–736.
- Morcos, S.A. (1970). Physical and chemical oceanography of the Red Sea. *Oceanography Marine Biology Annual Review*, **8**, 73–202.
- Neumann, A.C. and McGill, D.A. (1962). Circulation of the Red Sea in early summer. *Deep-Sea Research*, **8**, 223–235.
- Niitsuma, N., Oba, T. and Okada, M. (1991). Oxygen and carbon isotope stratigraphy at site 723, Oman Margin. *Proc. O.D.P., Scientific Results*, **117**, 321–341.
- Patzert, W.C. (1974a). Seasonal reversal in Red Sea circulation. *Centre National pour l'Exploitation des Océans (CNEXO), Actes de colloques*, **2**, 55–85.
- Patzert, W.C. (1974b). Wind-induced reversal in Red Sea circulation. *Deep-Sea Research*, **21**, 108–121.
- Pedgley, D.E. (1974). An outline of the weather and climate of the Red Sea. *Centre National pour l'Exploitation des Océans (CNEXO), Actes de colloques*, **2**, 9–23.
- Prell, W.L., Hutson, W.H., Williams, D.F., Bé, A.W.H., Geitzenauer, K. and Molfino, B. (1980). Surface circulation of the Indian Ocean during the last glacial maximum, approximately 18,000 years BP. *Quaternary Research*, **14**, 309–336.
- Reiss, Z., Luz, B., Almogi-Labin, A., Halicz, E., Winter, A., Wolf, M. and Ross, D.A. (1980). Late Quaternary Paleoceanography of the Gulf of Aqaba (Elat), Red Sea. *Quaternary Research*, **14**, 294–308.
- Rohling, E.J. (1994). Glacial conditions in the Red Sea. *Paleoceanography*, **9**, 653–660.
- Shapiro, G.I. and Meschanov, S.L. (1991). Distribution and spreading of Red Sea Water and salt lens formation in the northwest Indian Ocean. *Deep-Sea Research*, **38**, 21–34.
- Shimmiel, G.B. and Mowbray, S.R. (1991). The inorganic geochemical

- record of the northwest Arabian Sea: a history of productivity variation over the last 400 K.Y. from sites 722 and 724. *Proc. O.D.P., Scientific Results*, **117**, 409–429.
- Siedler, G. (1969). General circulation of water masses in the Red Sea. In: Degens, E.T. and Ross, D.A. (eds), *Hot Brines and Recent Heavy Metal Deposits in the Red Sea*, pp. 131–137, Springer, Berlin.
- Souvermezoglou, E., Metzl, N. and Poisson, A. (1989). Red Sea budgets of salinity, nutrients and carbon calculated in the strait of Bab-el-Mandab during the summer and winter seasons. *J. Marine Research*, **47**, 441–456.
- Tchernia, P. (1980). Descriptive regional oceanography. In: Swallow, J.C. (ed.), *Pergamon Marine Series*, Vol. 3.
- Thompson, E.F. (1939). Chemical and physical investigations: the exchange of water between the Red Sea and the Gulf of Aden over the 'sill'. *John Murray Expedition 1933–34. Science Reports*, **2**, 105–119.
- Thunell, R.C., Locke, S.M. and Williams, D.F. (1988). Glacio-eustatic sea-level control on Red Sea salinity. *Nature*, **334**, 601–604.
- van Campo, E., Duplessy, J.C. and Rossignol-Strick, M. (1982). Climatic conditions deduced from a 150-kyr oxygen isotope–pollen record from the Arabian Sea. *Nature*, **296**, 56–59.
- van der Linden, W.J.M., Zachariasse, W.J., Van der Weijden, C.H., *et al.* (1992). Shipboard report of NIOP cruise D2, October 4–November 25, 1992. Geological study of the Arabian Sea — Part 2, IPPU Internal Report, Utrecht.
- van der Weijden, C.H., Zachariasse, W.J., De Lange, G.J., Luther III, G.W., *et al.* (1992). Shipboard report of NIOP cruise D3, October 27–November 16, 1992, Geological Study of the Arabian Sea — Part 3, IPPU Internal Report, Utrecht University.
- Werner, F. and Lange, K. (1975). A bathymetric survey of the sill area between the Red Sea and the Gulf of Aden. *Geol. Jb.*, D13, 125–130.
- Winter, A., Almogi-Labin, A., Erez, Y., Halicz, E., Luz, B. and Reiss, Z. (1983). Salinity tolerance of marine organisms deduced from Red Sea Quaternary record. *Marine Geology*, **53**, m17–m22.
- Wyrki, K. (1971). *Oceanographic Atlas of the International Indian Ocean Expedition*. National Science Foundation, Washington DC, USA, 531 pp.
- Wyrki, K. (1973). Physical Oceanography of the Indian Ocean. In: Zeitzschel, B. (ed.) *The Biology of the Indian Ocean*, pp. 18–36, Springer-Verlag, New York.
- Zahn, R. and Pedersen, T.F. (1991). Late Pleistocene evolution of surface and mid-depth hydrography at the Oman margin: planktonic and benthic isotope records at site 724. *Proc. O.D.P., Scientific Results*, **117**, 291–308.